Rev. Adv. Mater. Sci. 42 (2015) 68-82

DISCRETE BREATHERS IN CARBON AND HYDROCARBON NANOSTRUCTURES

J.A. Baimova[1], E.A. Korznikova[1], I.P. Lobzenko[2] and S.V. Dmitriev[1,3]

[1]Institute for Metals Superplasticity Problems of RAS, Khalturina 39, Ufa 450001, Russia
[2]Institute of Molecule and Crystal Physics Ufa Research Center of RAS, Prospekt Oktyabrya 151, Ufa 450075, Russia
[3]Tomsk State University, Lenin Prospekt 36, Tomsk 634050, Russia

Received: April 09,2015

Abstract. Intrinsic localized modes or discrete breathers (DBs) are spatially localized, large-amplitude vibrational modes in defect-free nonlinear lattices. In this review, recent achievements in the investigation of properties of DBs in carbon and hydrocarbon nanostructures are discussed. After a brief overview of the carbon structures supporting DBs and special conditions for their excitation, the focus is placed on the discussion of properties of various DBs and their clusters in such materials. Then we speculate about the possible role of DBs in the formation of physical and mechanical properties of carbon and hydrocarbon nanomaterials.

1. INTRODUCTION

In recent decades, considerable interest has been sustained in the study of dynamical localization phenomena in spatially discrete systems, and particularly in the study of discrete breathers (DBs). DBs also termed as intrinsic localized modes (DBs), are localized excitations which can exist e.g. in one- [1-4], two- [3,5-10], and three-dimensional [10-13] lattices. In the pioneering theoretical works, they have been identified as exact solutions to a number of model nonlinear systems possessing translational symmetry [14-19]. Later, existence of DB was experimentally proved for a broad range of physical systems such as underdamped Josephson junction array [20], two-dimensional array of optical waveguides [21], quasi-one-dimensional biaxial antiferromagnet [22], Bose-Einstein condensate [23,24], one-dimensional micromechanical array of coupled cantilevers [25-27], two-dimensional nonlinear electrical lattices [28], to name a few. One of the interesting properties of DBs is that in some cases they have the ability to transport energy [29]. In fact, a targeted energy transfer between DBs can be achieved under certain conditions, which are illustrated in a clear but non-trivial manner in the nonlinear dimer [30]. By now it is understood that the concept of DBs is quite universal and that they should play an important role in nonlinear physical systems which define the importance of such studies.

Crystal lattices possess both the discreteness of atomic arrangement and the nonlinearity of interatomic interaction, and thus, they can, in principle, support the existence of DBs. The discovery of fullerenes, carbon nanotubes (CNTs) and graphene as novel carbon materials for nanotechnology [31,32] has attracted many efforts in the study of their unusual properties. Although, numerous properties of various carbon allotropes have been investigated for the last decade [33-37], still there is a lack of information, especially when describing the nonlinear dynamical properties of such structures. DBs in carbon materials were previously investigated for graphene [38-46], graphite [47], CNTs, fullerenes [48-

Corresponding author: J.A. Baimova, e-mail: julia.a.baimova@gmail.com

53] and hydrocarbons [54-57]. It was found that three types of strongly localized nonlinear modes (which are synonymous to DBs) can be found in CNTs [49]. The first type corresponds to longitudinal breathers with the frequencies in the range (1162, 1200) cm^{-1} which also exist in planar carbon structures. The second type, radial breathers, describes transverse localized nonlinear modes with the frequency band (562, 580) cm^{-1}. The third type, twisting breathers, characterizes localization of the nanotube torsion oscillations with the frequencies (1310, 1477) cm^{-1} [for the model with the Brenner potentials the twisting breathers have wider frequency spectrum, (1442, 1644) cm^{-1}].

Studies on DBs are highly important, for instance, for the understanding of mechanical instability, which is characterized by a bond switching. The latter can be closely connected with the localized modes. In general, the mechanical instability occurs at a local site where stress or strain concentrates due to the structural inhomogeneity. As for mechanical instability in the CNTs, a topological defect that consists of two pentagons and two heptagons coupled in pairs appears by the C-C bond rotation at a local site of the armchair CNTs under axial tension [58]. Remembering that the DB gives rise to the intensive energy concentration even in the absence of structural inhomogeneity by its localized vibration with large amplitude, one can assume a possibility that the excited DB in the armchair CNT could trigger the Stone-Wales transformation [52]. Nevertheless, such an interesting structure transformation has not been studied in the other carbon nanostructures, and that fact opens many opportunities for the investigation of DBs in graphene.

Experimental observations of discrete breathers in carbon nanostructures is a good challenge for future studies, because nowadays all works devoted to DBs in such structures are theoretical and done either by molecular dynamics (MD) simulation or by *ab initio* simulations (also refer to as “calculations from the first principles”). There are several interatomic potentials widely used for the simulation of carbon and hydrocarbon nanostructures. For example, let us notice the standard set of interatomic potentials that take into account valence bonds and angles between valence bonds, as well as torsion angles [59-62]. It was successfully used for solving different problems such as thermal conductivity of graphene stripes with rough edges, thermal conductivity of graphene nanotubes, properties of discrete breathers in graphene nanotubes, vibrational modes localized at the graphene edges. A distinctive feature of the potentials developed and used in [59-62] is that they reproduce some important characteristics of graphene, such as the dispersion curves, better than the well-known Brenner potential [63]. The Brenner empirical potential was developed, in particular, for studying the covalent-bond carbon-based materials and depends on the nearest neighbors of the considered atom. MD simulations of DBs in graphene can also be performed by means of the LAMMPS package [64] with the AIREBO potential [65], which was derived from reactive empirical bond-order Brenner potential [63]. The AIREBO potential can be used to model both chemical and intermolecular reactions in condensed-phase hydrocarbon systems, such as liquids, graphite and polymers. Brenner potential is very successful at describing intramolecular forces in carbon and hydrocarbon materials, while AIREBO potential also includes intermolecular interactions via 6-12 Lennard-Jones potential.

MD studies rely on the quality of interatomic potentials, which is always a question. For instance, in [64] it was shown that, among different interatomic potentials for the simulation of DBs in Si, only one (the Tersoff potential) can describe nonlinear properties in a proper way. The reason is that the interatomic potentials are often fitted to the elastic moduli and phonon spectra of crystals (calculated from *linearized* equations of motion) as well as to some experimentally measurable energies, such as the sublimation energy, vacancy energy, etc. (for which not the exact profile of the potential functions but their integral characteristics are important since the change in potential energy is path independent). On the other hand, DB, being an essentially *nonlinear* vibrational mode, is sensitive to the exact shape of the potentials. This suggests the importance of the *ab initio* simulations [55] of DBs in crystals. The first principle calculations (see ref. 38 from [55]) are based on the quantum-mechanical approach and, therefore, take into account the deformations of atoms electron shells during the DB oscillations. Thus, *ab initio* simulations are believed to be much more accurate then molecular dynamics with any empirical interaction potential.

In this review the phenomenon of DB and their possible role in carbon and hydrocarbon structures such as fullerenes, CNTs, graphene and graphane will be discussed. Open issues are raised and some perspectives of further studies on DBs are discussed.

2. DISCRETE BREATHERS IN GRAPHENE

It is important to consider at first the *linear* vibrational modes (so called eigenmodes) in graphene

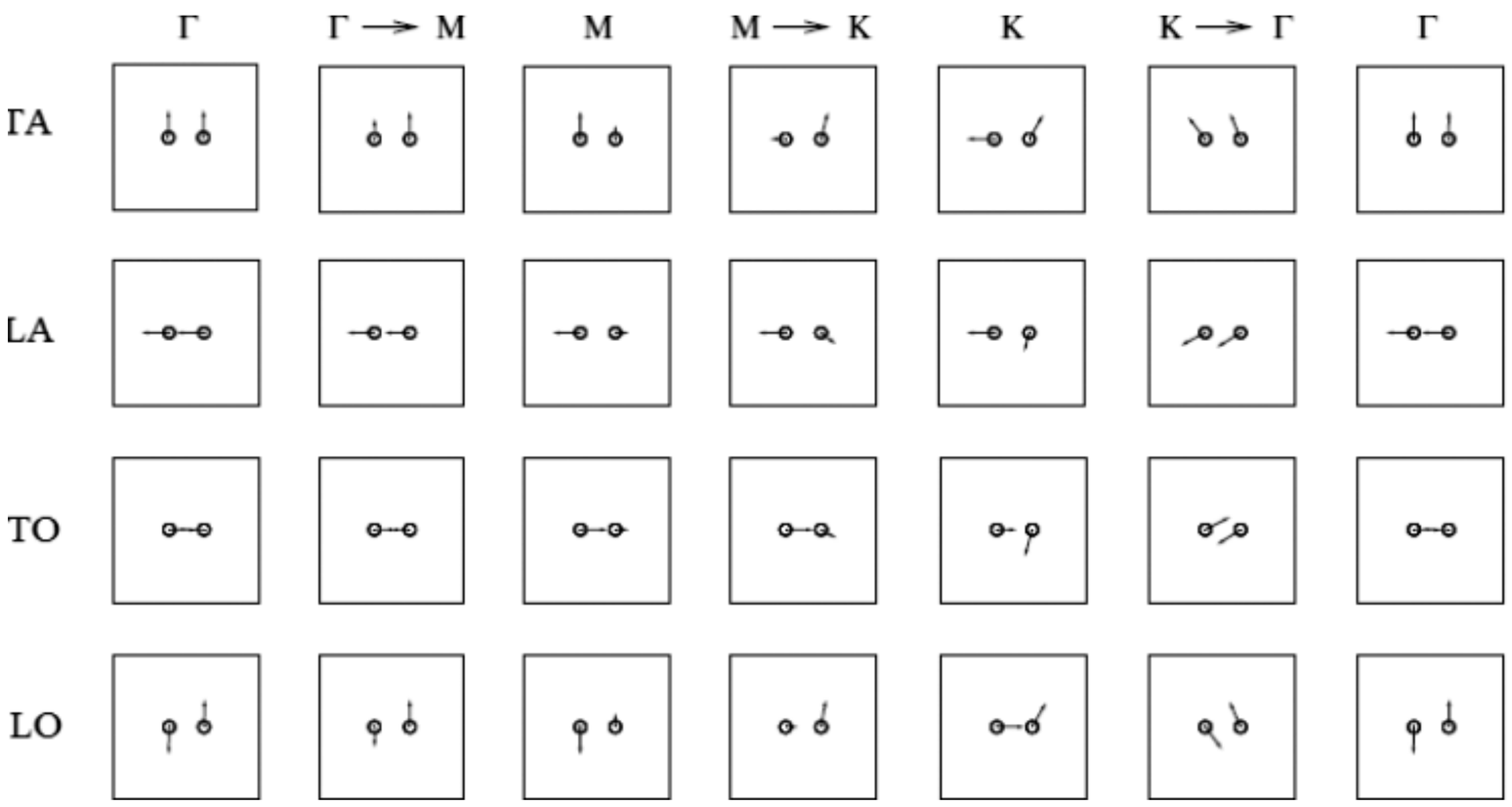

Fig. 1. Eigenmodes of the graphene sheet. Reprinted with the permission from Y. Yamayose, Y. Kinoshita, Y. Doi, A. Nakatani and T. Kitamura // *Europhys. Lett.* **80** (2007) 40008, © 2007 IOP Publishing.

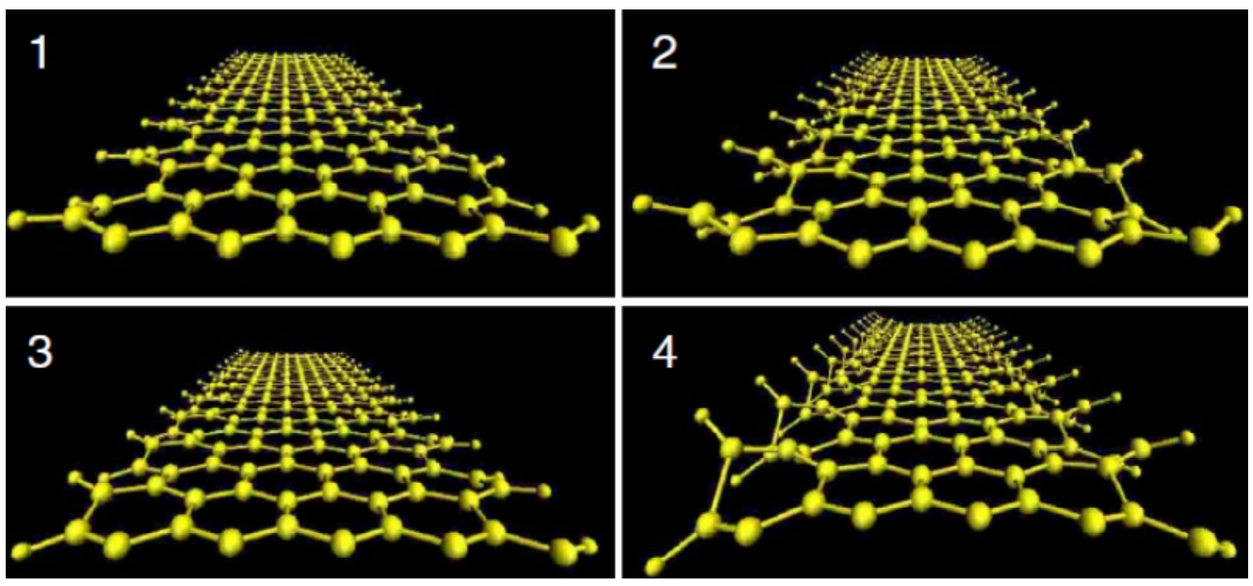

Fig. 2. Four snapshots displaying the 365 cm^{-1} edge-localized phonon mode at the armchair GNR saturated with hydrogens. Reprinted with the permission from M. Vandescuren, P. Hermet, V. Meunier, L. Henrard and Ph. Lambin // *Phys. Rev. B* **78** (2008) 195401, © 2008 American Physical Society.

despite they are quite different from the nonlinear excitations such as DBs. The analysis of eigenfrequencies and eigenmodes in graphene has been done in [38]. Fig. 1 shows the eigenmodes for branches *TA*, *LA*, *TO,* and *LO* of graphene dispersion curves. Letters K, M, and Γ denote the high-symmetry points of the first Brillouin zone in the reciprocal space. The round marks indicate the two atoms in the primitive cell of graphene sheet and the arrows denote the eigenvectors. *TA* and *LA* branches, in which the two atoms move in the same directions with the same displacement, depict the translation of the entire system. Essentially, these modes differ from the DB because they are in-phase vibrations. The shape of the nonlinear vibrational mode that corresponds to DB can be similar to one of the linear eigenmodes of the system. The difference between them is that in the linear modes all atoms vibrate with the same amplitude while the DB exhibits spatially localized vibration of some atoms.

The majority of the experiments are devoted to the investigations of the properties of graphene nanoribbons (GNR), because practically it is much easier to produce nanoribbons instead of large graphene sheets. It has been recently shown that a GNR can be peeled off from the topmost layer of highly oriented pyrolytic graphite by scanning tunneling microscope lithography operated in air, allowing the design of arbitrary geometry. Because of the presence of edges on both sides, GNRs possess a set of particular properties, depending on width and helicity. The intrinsic phonon modes, of GNRs which cannot be excited for graphene sheet were studied in [46] both by MD and first principle calculations. Several types of phonon modes were found both for zigzag and armchair GNRs. The examples are shown in Figs. 2 and 3. The real-space representation of the phonon displacement eigenvectors of these two modes allows us to assign the mode calculated at 365 cm^{-1} to an out-of-plane edge-localized motion of the carbon atoms (see Fig. 2). At higher frequencies, a characteristic zigzag GNR

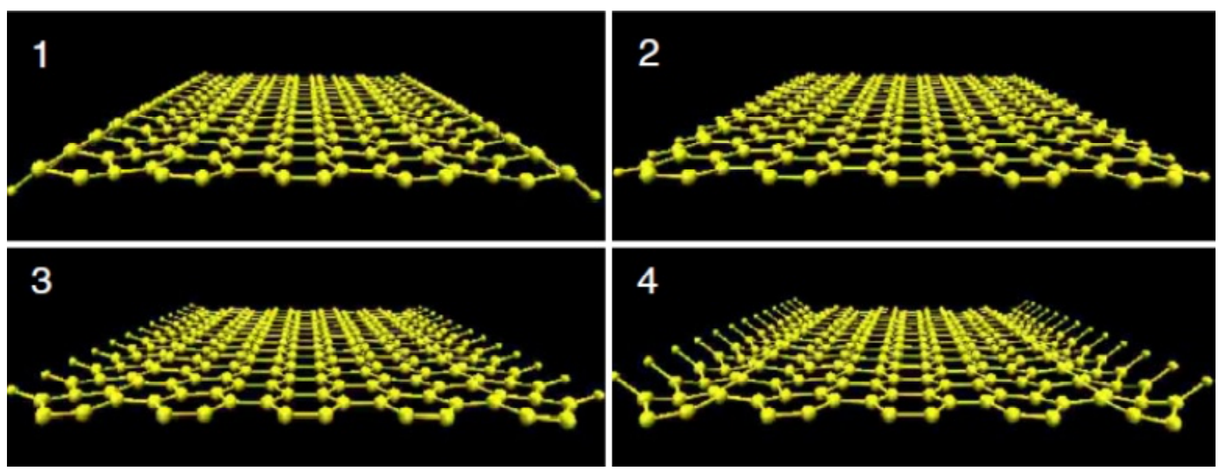

Fig. 3. Four snapshots displaying the 610 cm^{-1} edge-localized phonon mode at the zigzag GNR saturated with hydrogens. Reprinted with the permission from M. Vandescuren, P. Hermet, V. Meunier, L. Henrard and Ph. Lambin // *Phys. Rev. B* **78** (2008) 195401, © 2008 American Physical Society.

mode centered around 610 cm^{-1} was found (see Fig. 3).

Radial breather-like modes were studied in [66] by means of first principle calculations for GNRs of small width and in [67] by MD simulations with empirical Brenner potential for wide GNRs. It was found that the radial breather-like mode frequencies of GNRs of different widths follow two different rules. For the wide GNRs whose widths are larger than 25 Å, breathers frequencies follow a new $1/w$ rule: $\omega = 3086.97\times(1/w)+1.08$. But for the narrow GNRs whose widths is less than 25 Å, frequencies follow the $\sqrt{1/w}$ rule: $\omega = 1407.81\times\sqrt{1/w}-164.38$, for which the original simple 1D oscillator model is correct. Finally, a unified fitting function was obtained, which can be suitable for all the GNRs, from narrow to wide ones. All these rules provide a possible experimental method to determine the GNR width by Raman spectra.

The other interesting point is the investigation of vibrational modes near defects. Despite the definition of DBs does not include vibrational modes on defects, some attention should be devoted to this issue in the frames of discussion of vibrational modes in graphene. Peculiar vibrational modes of graphene nanoribbons (GNRs) with topological line defects were presented in [68]. It was found that phonon dispersion relations of the topological defective GNRs are more similar to those of perfect armchair-edge GNR than to zigzag-edge GNR in spite of their zigzag edge. Three types of characteristic vibrational modes, namely, localized vibrational modes on defect sites, edge modes, and breathing modes were observed. It was shown that the edge modes are related to the structural symmetry but not to the nanoribbon widths.

It is well-known that in the structures with the gap in the phonon spectrum the so-called gap DBs (i.e. the DBs having frequency within the phonon gap) can be excited [13]. Elastic strain engineering is a promising way to modify and control properties of nanomaterials and can be successfully applied to change the phonon density of states of some nanostructures [69-74]. The possibility of excitation of gap DBs in graphene was studied in [42]. Dispersion curves of unstrained graphene which contain three acoustic and three optical branches are given

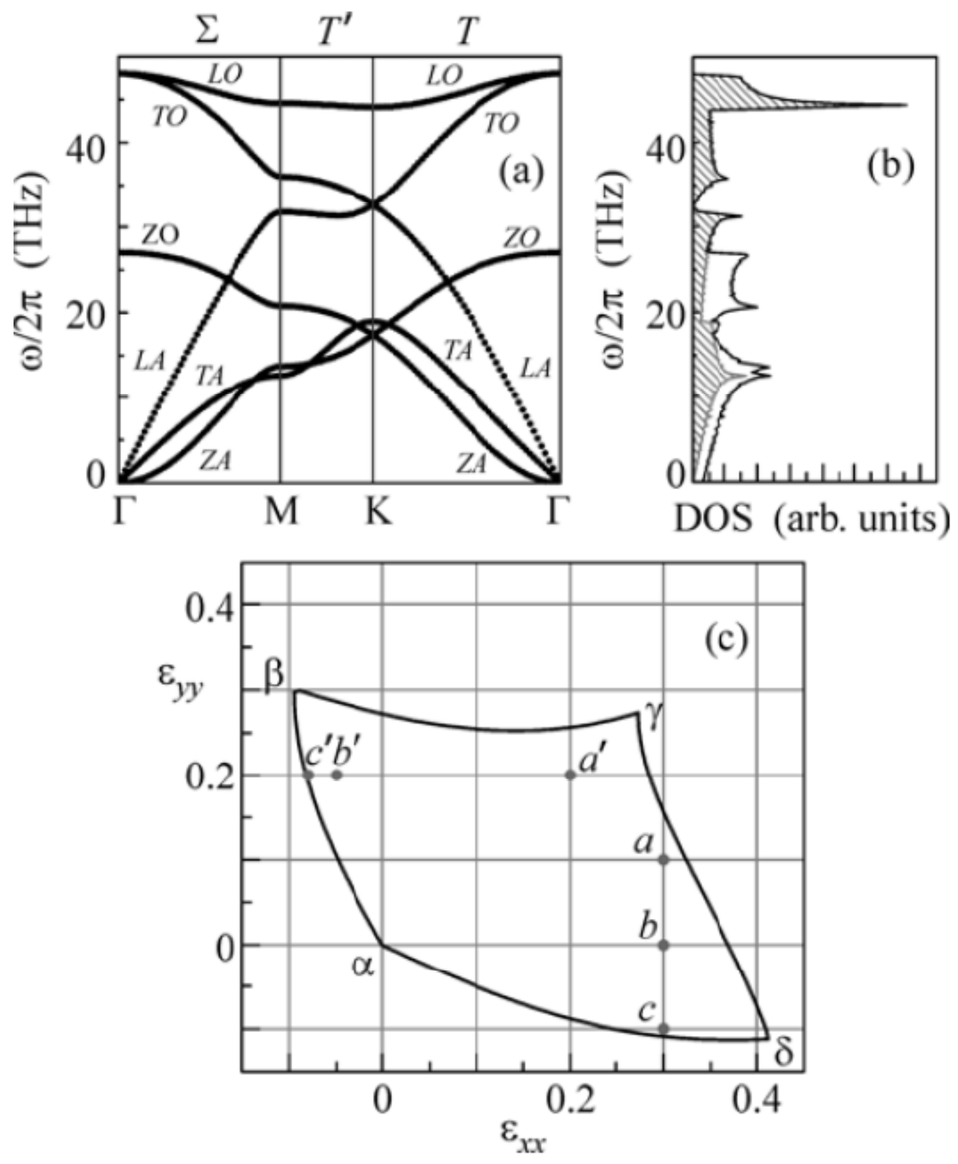

Fig. 4. (a) Dispersion curves of unstrained graphene. Acoustic modes *LA* and *TA* correspond to the longitudinal and transverse oscillations in the graphene plane, respectively. The acoustic wave *ZA* describes the transverse oscillations normal to the graphene sheet. (b) DOS of unstrained graphene. The shaded DOS does not include modes that have only *z* components of the atomic displacements (*ZA* and *ZO*). (c) Stability region of orthotropic graphene in the deformed state with $\varepsilon_{xx} \neq 0$, $\varepsilon_{yy} \neq 0$, and $\varepsilon_{xy} = 0$. Reprinted with the permission from L.Z. Khadeeva, S.V. Dmitriev and Yu.S. Kivshar // *JETP Lett*. **94** (2011) 539, (c) 2011 © Springer.

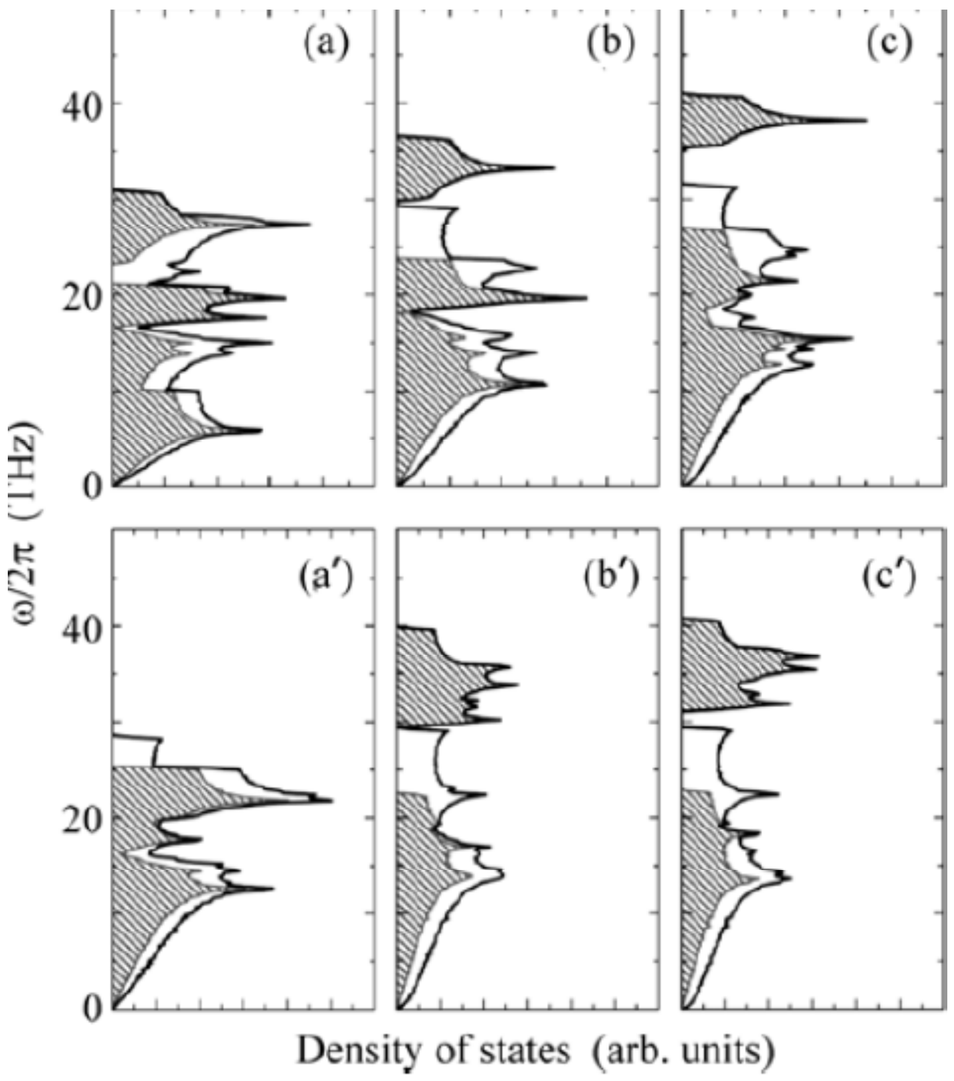

Fig. 5. (a) Effect of the elastic deformation of graphene on DOS for ε_{yy} equal to (a) 0.1, (b) 0, and (c) -0.1 at the given ε_{xx} = 0.3 and ε_{xy} = 0; and for ε_{xx} equal to (a') 0.2, (b') -0.05, and (c') -0.08 at the given ε_{yy} = 0.2 and ε_{xy} = 0. Panels from (a) to (c) correspond to the strains denoted in Fig. 4c by the points from *a* to *c* and panels from (a') to (c') correspond to the strains denoted in Fig. 4c by the points from *a*' to *c*'. The shaded DOS do not include the frequencies of the phonons oscillating normal to the plane of the graphene sheet, i.e., the frequencies of the *ZA* and *ZO* modes. Reprinted with the permission from L.Z. Khadeeva, S.V. Dmitriev and Yu.S. Kivshar // *JETP Lett*. **94** (2011) 539, (c) 2011 © Springer.

in Fig. 4a. The acoustic branches with the highest (*LA*) and intermediate (*TA*) frequencies correspond to the longitudinal and transverse waves in the plane of the graphene sheet, respectively. The low-frequency acoustic wave (*ZA*) corresponds to the transverse waves out of the plane of the graphene sheet. The density of phonon states (DOS) of unstrained graphene is presented in Fig. 4b. It was shown that in the unstrained graphene only DBs having frequencies above the phonon band can be found [38,43]. Basic properties of the DB in graphene based on precise numerical solutions of DBs were studied by means of MD simulations. The structure of the DB obtained by the iteration method (see [43] for more details) indicates the existence of some nonlinear intrinsic properties: large amplitude vibration, frequency dependence on amplitude, and asymmetric structure of amplitude. The *numerically exact* DB having frequency greater than the maximum frequency of the phonon band was found to be *always linearly unstable* [38,43].

Application of uniaxial tension opens a gap in the spectrum of graphene [42,71,72,75] and the so-called gap DBs, having frequencies within the gap, can be easily excited [24]. From Fig. 4b it can be seen that the phonon spectrum of graphene has no gaps. Knowing the deformation stability region (see Fig. 4c), one can try to find the DBs in the strained graphene [71,73,74]. DOS studied in [42] contains the gap of different width depending on the applied strain (see Fig. 5). It was shown that a wide gap can be found, e.g., for ε_{yy}=-0.1 and ε_{xx}=0.3, ε_{xy}=0 (see Fig. 5c). Authors of [42] have succeeded in the excitation of gap discrete breathers, stroboscopic picture of which is shown in Fig. 6a. It can be seen that DB in graphene has two neighboring carbon atoms oscillating in the antiphase along the *y* axis, i.e., along the armchair direction. It was also shown

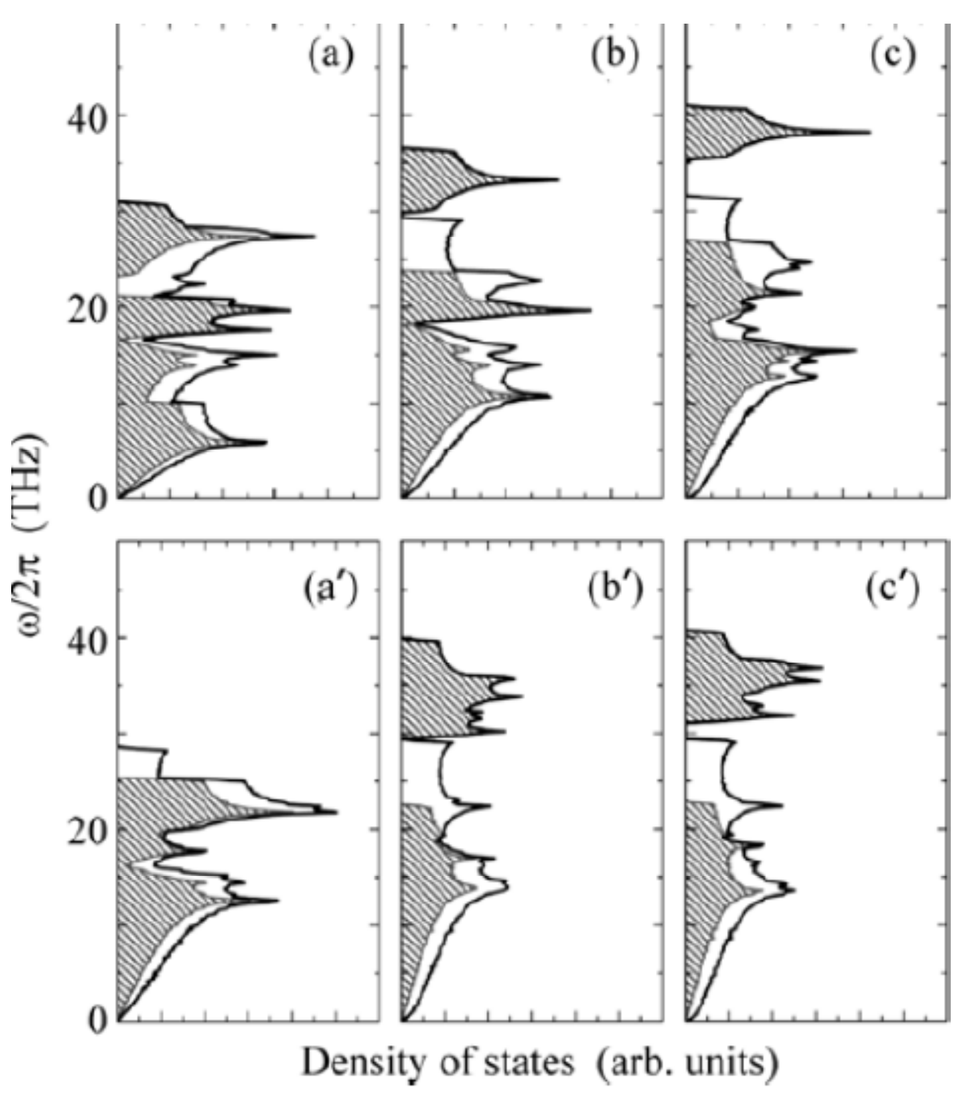

Fig. 6. (a) Stroboscopic pattern of the motion of atoms in the vicinity of the discrete breather in graphene subjected to the elastic strain ε_{xx} = 0.35, ε_{yy} = -0.1, and ε_{xy} = 0. (b) DOS including and (shaded) not including the *ZA* and *ZO* modes and the frequency of the discrete breather versus its amplitude *A* (dots connected with the line). (c) The *y* component of the displacements of the two atoms of the discrete breather versus the dimensionless time t/Θ, where Θ is the period of the oscillation of the discrete breather. Reprinted with the permission from L.Z. Khadeeva, S.V. Dmitriev and Yu.S. Kivshar // *JETP Lett*. **94** (2011) 539, (c) 2011 © Springer.

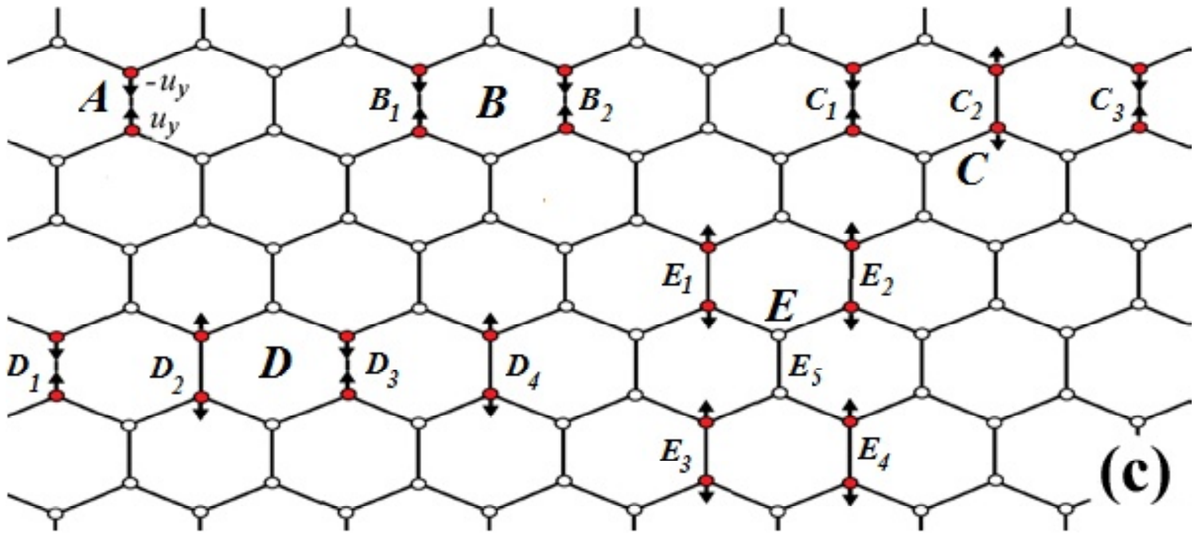

Fig. 7. A single DB (A) and the DB clusters containing two (B), three (C), and four (D and E) DBs. DBs within the clusters are numbered. Reprinted with the permission from J.A. Baimova, S.V. Dmitriev and K. Zhou // *Europhys. Lett.* **100** (2012) 36005, (c) 2012 IOP Publishing.

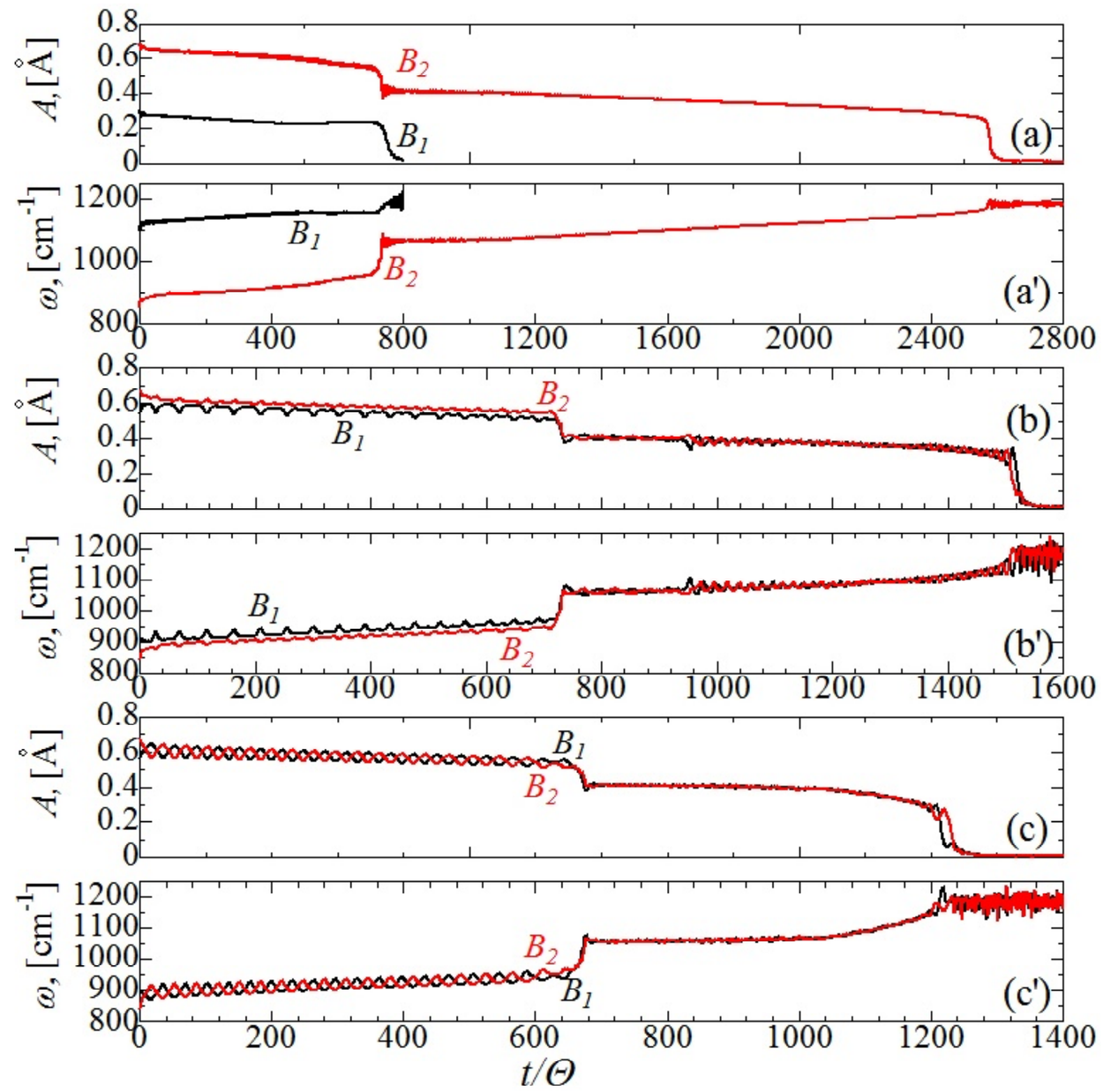

Fig. 8. Amplitudes, *A*, and frequencies, ω, of B_1 and B_2 (see Fig. 7) for the DB pairs excited with the different initial conditions (a), (a') different initial amplitudes; (b), (b') initial amplitudes close to each other; and (c), (c') equal initial amplitudes. Reprinted with the permission from J.A. Baimova, S.V. Dmitriev and K. Zhou // *Europhys. Lett.* **100** (2012) 36005, (c) 2012 IOP Publishing.

that considered DB is a long-living oscillation of atoms, stable to the small perturbations. Fig. 6b shows the gap in phonon spectrum with the dependence of the amplitude of DB on its frequency. The dashed area in Fig. 6b shows the phonon spectrum excluding the frequencies of phonons oscillating out of the graphene plane, i.e., *ZA* and *ZO* modes. The *y* component of the atoms displacements is shown in Fig. 7c as a function of the dimensionless time t/Θ, where $\Theta = 0.033$ ps is the period of the oscillation of the discrete breather.

DB clusters is the other interesting point in the investigation of DBs in carbon structures because they can localize a larger amount of energy than a single DB. This energy can be spent, for example, to create a defect of crystal lattice, as it was demonstrated in the case of CNTs under axial tension [52]. DBs as well as their clusters can also be spontaneously excited in crystals at finite temperatures [76,77], and then assist crack initiation and fracture of graphene under applied tension. The energy exchange between DBs in clusters shown in Fig. 7 was studied in [40] using the standard set of interatomic potentials.

In Figs. 8a and 8a', respectively, the amplitudes and the frequencies of B_1 (left breather in the clus-

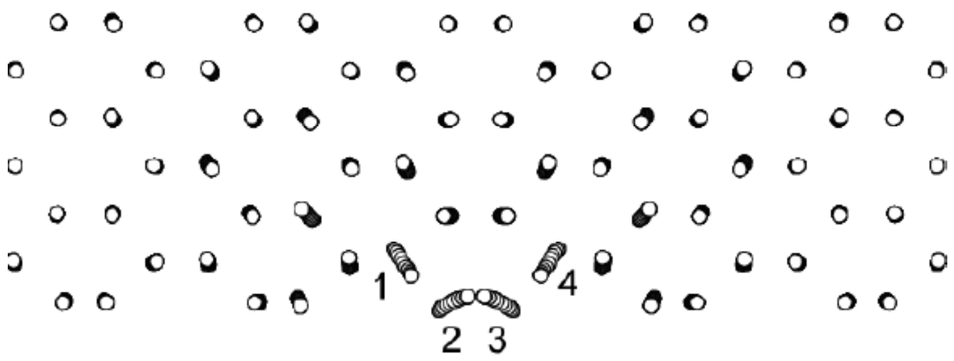

Fig. 9. Stroboscopic picture of DB at the edge of the armchair GNR. Reprinted with the permission from E.A. Korznikova, J.A. Baimova and S.V. Dmitriev // *Europhys. Lett.* **102** (2013) 60004, © 2013 IOP Publishing.

ter B in Fig. 7) and B_2 (right breather in the cluster B in Fig. 7) are shown for the considered DB pair as the functions of dimensionless time (*t*/Q, where Q is the breather period), respectively. It can be seen that in this DB pair, the initial amplitude of B_1 is rather small and it disappears after about 700 oscillation periods. On the other hand, B_2, having larger initial amplitude, survived until 2600 *t*/Q. In Figs. 8b,8b' and 8c,8c' the same as in Figs. 8a and 8a' is shown, but for the other initial conditions. In case when the amplitudes and the frequencies of the two DBs in the pair are close, the periodic detuning of oscillation phases of the DBs results in a partial energy exchange between DBs until 700 oscillation periods. After the burst of energy and amplitude reduction, both DBs have nearly the same amplitudes and they disappear *simultaneously*. In the case with equal DB's amplitudes, the energy exchange between DBs took place (Figs. 8c,8c'). Effect of energy exchange which appeared at some conditions is of high importance in terms of structure transformations, because such energy redistribution can lead to various effects like defect nucleation, fracture, to name a few. All the other DB clusters show similar behavior with quite active energy exchange. Interesting scenario was found for case E (see Fig. 7) when four initially exited DBs transfer their energy to DB E_5.

DBs were also found at the edge of strained armchair GNRs [39, 41]. An example of DB at the edge of the nanoribbon under a tensile strain of ε_{xx}=0.15 is shown in Fig. 9 by the stroboscopic picture of atomic motion where displacements of atoms from their lattice positions are multiplied by a factor 3. Such a DB consists of four carbon atoms vibrating at the edge of GNR as it is shown in Fig. 9. DB is the vibrational mode with atoms moving in the XY-plane which does not interact with the Z-modes even though it has frequencies within the Z-mode phonon spectrum. For small amplitudes of atoms vibrations the DB frequency bifurcates from the frequency of

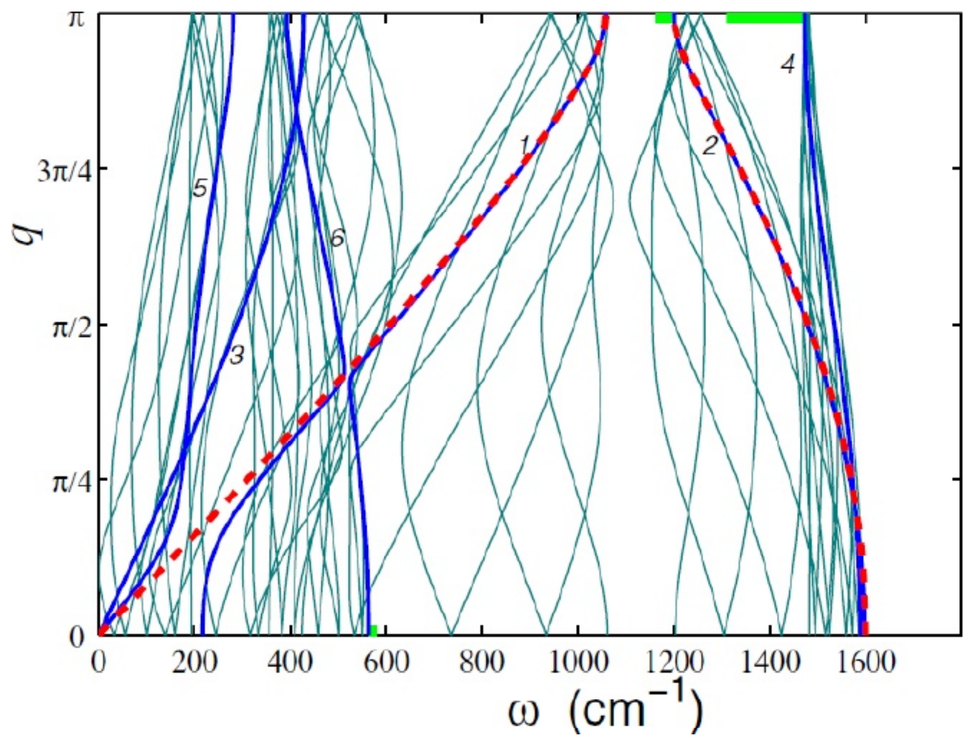

Fig. 10. Sixty dispersion curves of the CNT phonon modes: acoustic (1) and optical (2) longitudinal, acoustic (3) and optical (4) rotation, acoustic (5) and optical (6) radial phonons. Reprinted with the permission from A.V. Savin and Y.S. Kivshar // *Europhys. Lett*. **82** (2008) 66002, (c) 2008 IOP Publishing.

the phonon mode localized at the nanoribbon edge and decreases with the increase of the amplitude demonstrating soft-type anharmonicity. It is believed that such a DBs can play an important role in the thermally activated fracture of GNRs under tension.

3. DISCRETE BREATHERS IN FULLERENES AND CARBON NANOTUBES

Excitation of DBs in CNTs with chiralities (*m*,0) and (*m*,*m*) was investigated in [49]. A simple form of the Hamiltonian allows one to obtain analytical results for the nonlinear dynamics similar to the case of diatomic lattices, which predict the existence of DBs with the frequencies below the lowest frequency of the longitudinal phonons (Fig. 10). The breather form is shown in Fig. 11. Its frequency is inside the band (1162,1200) cm^{-1} near the lowest edge of the longitudinal optical oscillations. Three types of DBs were found: longitudinal, radial and twisting breathers.

The longitudinal breathers become coupled to the transverse phonon modes, and they emit radiation. This radiation is defined by the curvature of the nanotube and the index *m*. Therefore, the longitudinal breathers are not genuine nonlinear modes of carbon nanotubes, and they possess a finite lifetime. The second type of discrete breathers is associated with the localization of transverse radial oscillations of a nanotube. Example of this radial breather in the nanotube (10,0) is shown in Figs. 11b and 11d. Localized out-of-phase transverse os-

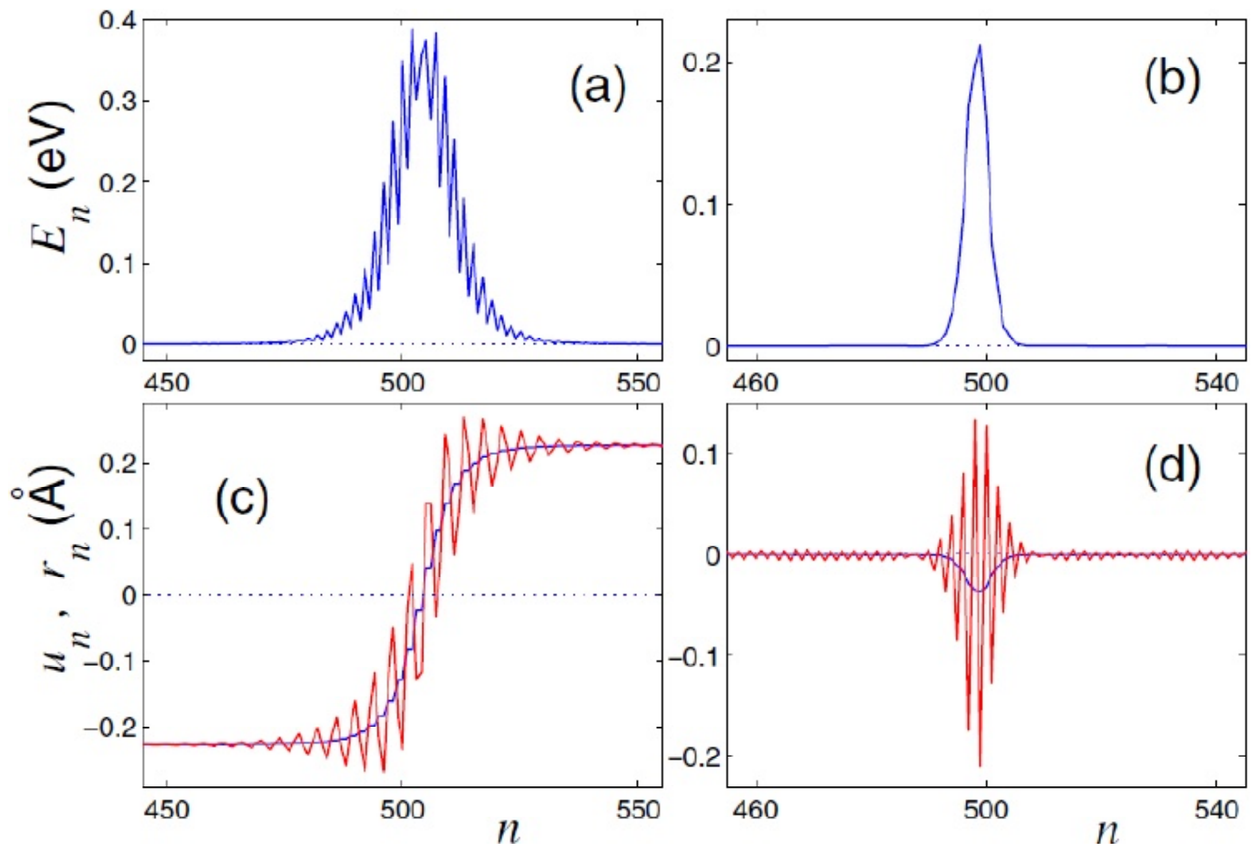

Fig. 11. (a,c) Example of a localized nonlinear mode for the longitudinal oscillations, and (b,d) example of a radial breather describing localization of the transverse vibrations of a nanotube (10,0). Shown are: (a,b) averaged (in time) energy distribution E_n in the chain, (c) atom displacements u_n, and (d) transverse displacements r_n. In (c,d) blue lines show the values averaged over the period, red ones show maximal displacements. Radiation of longitudinal waves by a radial breather is visible in (d). Reprinted with permission from A.V. Savin and Y.S. Kivshar // *Europhys. Lett*. **82** (2008) 66002, (c) 2008 IOP Publishing.

cillations of the neighboring atoms lead to localized contraction and extension of the nanotube. Such transverse oscillations become coupled to the longitudinal oscillations and, therefore, the radial breathers radiate longitudinal phonons. As a result, the radial breathers are also not genuine nonlinear localized modes of the carbon nanotubes, and they decay slowly by emitting small-amplitude phonons [49]. The lifetime of these breathers can be of the order of several nanoseconds. The third type is a twisting breather, associated with the torsion oscillations of the nanotube. The twisting breather is an exact solution of the motion equations of the nanotube, and it does not radiate phonons.

The atomic study was extended to a quasi-three-dimensional (3D) system of a carbon nanotube (CNT), which is made by rolling up a graphite sheet in a specific direction. Unlike the graphite sheet, CNTs characteristically have a variety of microscopic structures depending upon the rolling direction (chirality). Kinoshita et al. [48] conducted molecular dynamics simulations for two typical chiralities, the zigzag and armchair CNTs, and demonstrated a distinct difference in the excitation of DBs. The DB can be excited in the zigzag CNTs but not in the armchair CNTs. Although understanding the mechanism of DB excitation in CNTs is essential for the nature of DBs as well as the mechanical behavior of CNTs [52], it has not yet been thoroughly elucidated. In addition, the chiral samples were too limited to profoundly discuss the selective mechanism, as the previous study [48] addressed only two examples, zigzag and armchair CNTs, which have no helicity.

The molecular dynamics simulations of various CNTs with different chirality in order to reveal the selective mechanism of excitation or non-excitation of the DBs was conducted in [50]. In the previous studies of a graphite sheet and a zigzag CNT [38,48], the DB was successfully generated by initially applying a displacement that corresponds to the zone boundary phonon mode and a momentum for a minute disturbance. Fig. 12a shows the simulation models of (8,0) zigzag, (6,3), (3,6), (7,1) chiral, and (5,5)A and (5,5)B armchair CNTs considered in [50]. The orientation of initial displacement for each CNT (vibration angle, y, which is defined as the angle from the axial *z* direction, is shown in Fig. 12b. It was shown that, the DB cannot be excited in the latter ((3,6), (7,1), and (5,5)B CNTs) because of their weaker nonlinearity in comparison with (8,0), (6,3), and (5,5)A CNTs. Thus, the selective excitation of DBs is governed by the nonlinearity of the C-C interaction. Furthermore, nonlinearity dominates the characteristics of DBs; frequency and lifetime of the DB increase as nonlinearity becomes stronger [50].

The importance of DBs for structural transformations was shown in [52], where the armchair CNT was studied by means of MD simulations. Computer experiments were conducted for a (5,5) armchair CNT under axial tension with the aim to elucidate the role of DBs in the atomic scale, as a possible trigger of the Stone-Wales transformation that

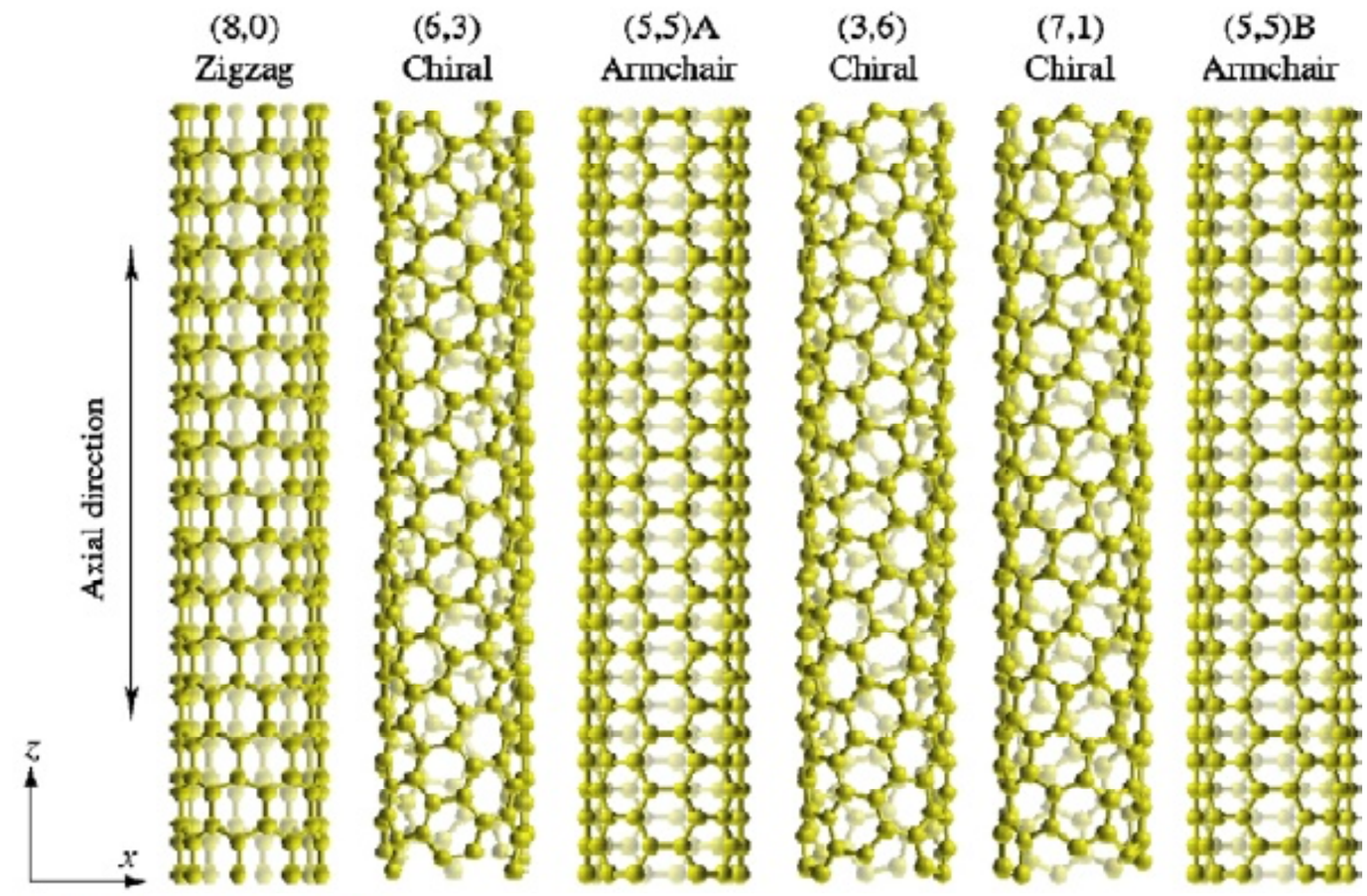

Fig. 12. (a) Simulation models of zigzag, chiral, and armchair CNTs. (b) Initial condition of atomic displacements for each CNT. The ψ represents the angle between the displacement vector and the axial direction (vibration angle). Reprinted with the permission from T. Shimada, D. Shirasaki, Y. Kinoshita, Y. Doi, A. Nakatani and T. Kitamura // *Physica D* **239** (2010) 407, (c) 2010 Elsevier.

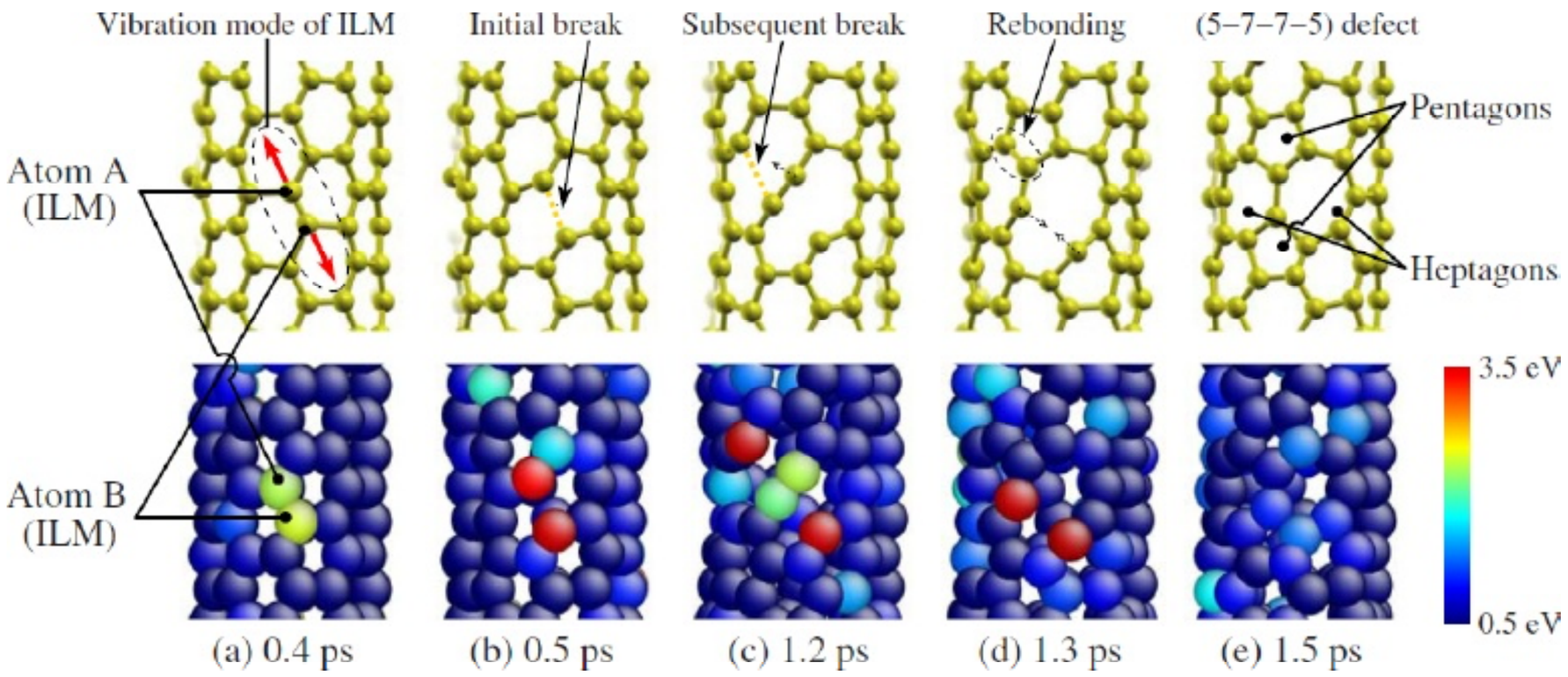

Fig. 13. Change in atomic configuration (top) and distribution of total energy of an atom, E_i, (bottom) during 0.4–1.5 ps. Only the vicinity of the DB-excited atoms A and B is shown for clarity. The red (gray) arrows at 0.4 ps indicate the vibrations of the DB. Reprinted with the permission from T. Shimada, D. Shirasaki and T. Kitamura // *Phys. Rev. B* **81** (2010) 035401, © 2010 American Physical Society.

locally produces a topological defect consisting of two pentagons and two heptagons coupled in pairs (5-7-7-5). A strong vibration of a pair of neighboring atoms was observed at a local site of the CNT, where kinetic energy concentrated and this state continued for several hundred femtoseconds (see Fig. 13). The excited DB was gradually amplified by the nonlinearity of C-C interaction, which always plays a central role in determining the excitation and fundamental properties of the DBs. The amplified DB vibration, finally, induced a C-C bond breaking at the excitation site that leads to the Stone-Wales

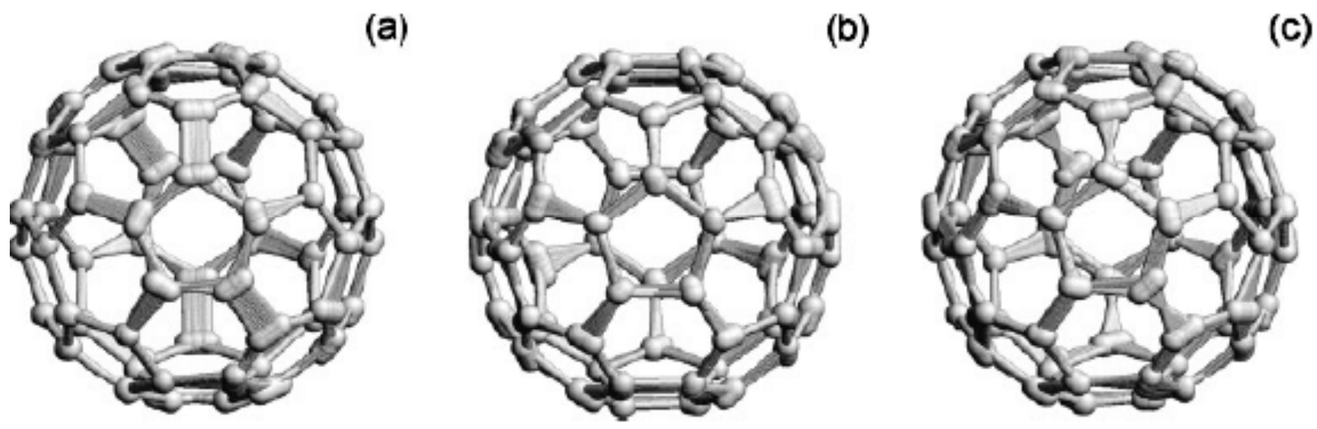

Fig. 14. Selected eigenmodes of an isolated C_{60} molecule, which lead to the generation of spatially localized nonlinear modes (breathers) of the fullerene crystal. (a) mode $T_{3g}(1)$ (frequency $\omega = 442.3$ cm^{-1}); (b) mode $T_{1g}(2)$ (frequency $\omega = 675.7$ cm^{-1}); (c) mode $T_{1g}(3)$ (frequency $\omega = 1454.9$ cm^{-1}). Reprinted with the permission from A.V. Savin and Y.S. Kivshar // *Phys. Rev. B* **85** (2012) 125427, © 2012 American Physical Society.

transformation because the intense energy concentration by the DB exceeded the activation barrier. In other words, the highly amplified DB triggered the mechanical instability of the Stone-Wales transformation in the (5,5) CNT under axial tension. This atomic-level mechanism, DB-derived mechanical instability, can be universally applicable to other situations. For example, it may be an origin of phase transformation in silicon under hydrostatic pressure or multiaxial stress. Further study of the connection between the DBs and the mechanical instability will be performed in the near future.

Fullerite C_{60} in the solid state is a typical molecular material in which the molecules are weakly bound together by van der Waals forces, and the electronic excitations are very close in energy and nature to those of the free molecule. As well as the other carbon nanostructures fullerenes with its unique properties are of great interest. By now, many structural, electronic, and vibrational properties of fullerenes have been studied in detail. In spite of the rapidly growing interest in new forms of fullerenes, icosahedral C_{60} remains at the focus of active research as a prototype fullerene system. It was revealed that composite nanostructures composed of fullerenes C_{60} can support long-lived strongly localized nonlinear modes, which resemble discrete breathers in simple nonlinear lattices [53] (see Fig. 14). For such modes, the kinetic energy is localized primarily in the rotational modes of a single C_{60} molecule and it decays slowly inside the fullerene nanocrystal. The existence of such long-lived localized nonlinear states in the nanoclusters explains the anomalously slow thermal relaxation observed in such structures when the temperature gradient decays in accord with the power, but not exponential, law, thus violating the Cattaneo-Vernotte law of thermal conductivity.

4. DISCRETE BREATHERS IN HYDROCARBONS

Although graphite is known as one of the most chemically inert materials, it was found that graphene can react with many atoms, e.g., with atomic hydrogen, which transforms this highly conductive zero-overlap semimetal into a semiconductor. The fully hydrogenated graphene, named graph**a**ne (see Fig. 15a), was first theoretically predicted [78, 79] and then experimentally confirmed by Elias et al. [80]. Unlike graphene, graphane is no longer planar but crumpled because hydrogen atoms are bonded to all the carbon atoms on both sides of the plane alternatively and the hybridization of carbon atoms is transformed from sp^2 to sp^3. As it can be seen from Fig. 15b, there is a wide gap in the density of the phonon states, which defines the opportunity to excite DB in graphane. DB can be excited by displacing a single hydrogen atom along the out-of-plane direction as it is shown in Fig. 15c. When H_0, being displaced from the equilibrium position, is released, most of the system energy remains localized in the form of a DB, while the rest of the energy is transferred to the other atoms of the graphane sheet (background atoms) through C_0, the first atom excited by H_0, resulting in their vibrations or the so-called 'background vibrations'. These vibrations would disturb the DB and affect its stability or lifetime. In fact, one needs the "perfect" profile of initial displacements of *all* atoms to induce *exact* discrete breather in the system. Otherwise the localized dynamical object would not be strictly periodic in time and should be called *quasi-breather* [81]. The problem of refining the initial displacements profile which corresponds to the DB in graphane was discussed in [82].

DBs in graphane were studied both by MD and *ab initio* simulation. In MD model it was shown that

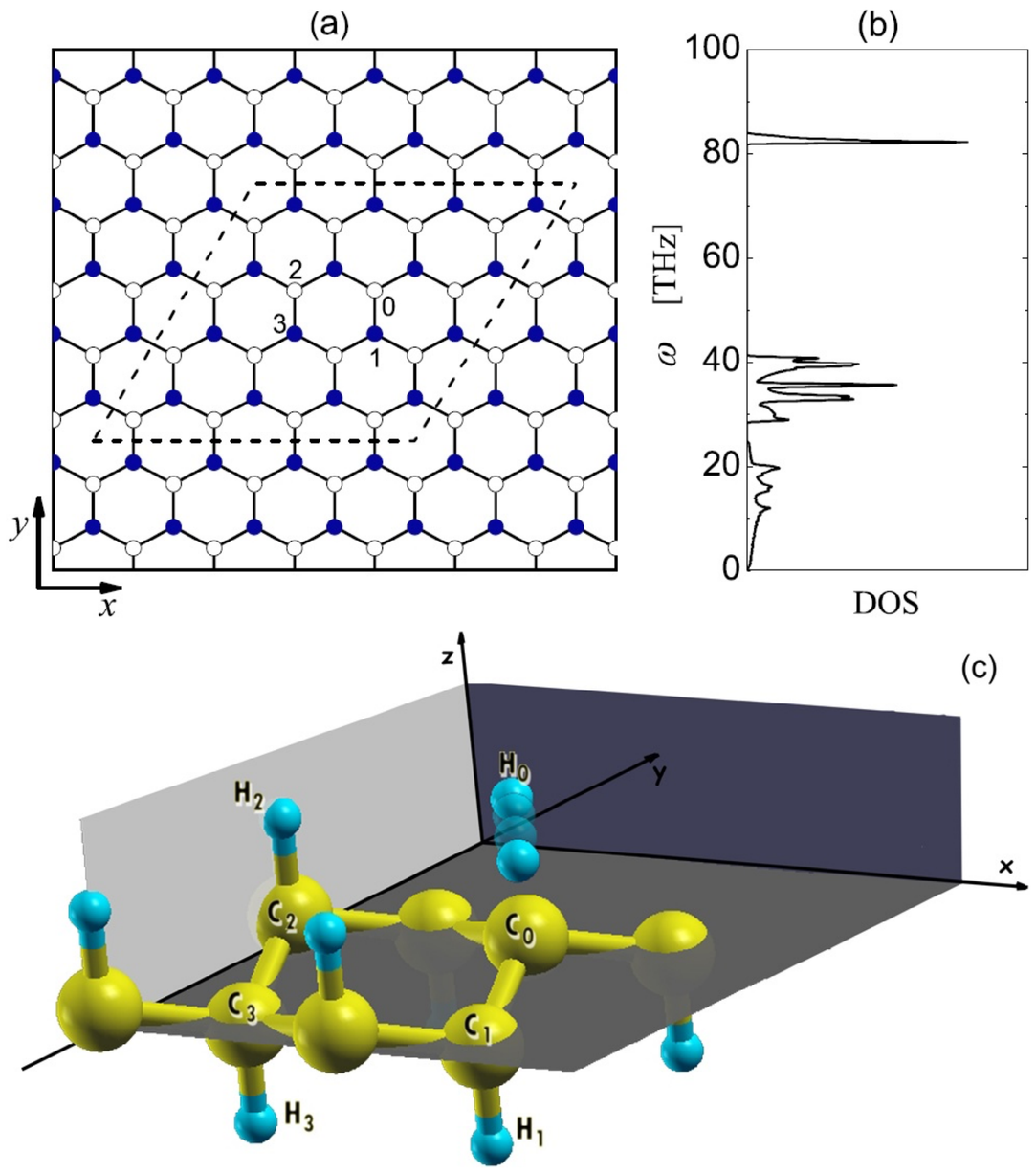

Fig. 15. (a) Structure of graphane (chemical formula - CH). Open (filled) dots show carbon atoms with hydrogen atoms attached above (below) the sheet. (b) phonon DOS of graphane. (c) Schematic presentation of the DB in graphane. The H_0 atom vibrates with a large amplitude while all other atoms have much smaller vibrational amplitudes. Reprinted with the permission from G.M. Chechin, S.V. Dmitriev, I.P. Lobzenko and D.S. Ryabov // *Phys. Rev. B* **90** (2014) 045432, © 2010 American Physical Society.

the frequency ω_D of the DB depends on its amplitude, as presented in Fig. 16 where ω_D=1/Q [54]. The lower(solid) and middle (dotted) horizontal lines delineate the lower (56.92 THz) and upper (87.83 THz) bounds of the phonon spectrum gap, respectively, while the upper (dashed–dotted) line delineates the upper bound (88.70 THz) of the whole spectrum. The $\omega_D(A)$ curve can be divided into three regions: (i) a soft-type anharmonicity of the DB, (ii) a hard-type anharmonicity, which has rarely been observed in realistic crystal models and (iii) a soft-type anharmonicity again. In region I, the frequencies of the DBs lie within the gap of the phonon spectrum; in regions II and III, they are located below the upper bound of the whole phonon spectrum when 0.17 Å<*A*<0.2 Å and above the upper bound when *A*>0.2 Å. In Fig. 17 the DB frequency ω_{DB} as the function of amplitude *A* is given from *ab initio* simulations in the framework of the density functional theory (see [55] and Ref. 38 from it). Edges of the phonon DOS gap are shown by the horizontal dashed lines. It can be seen that the $\omega_{DB}(A)$ curve bifurcates from the upper edge of the phonon gap and then decreases almost linearly with increase in *A*, entering the lower phonon band. The decrease in frequency with increase in amplitude reveals a soft-

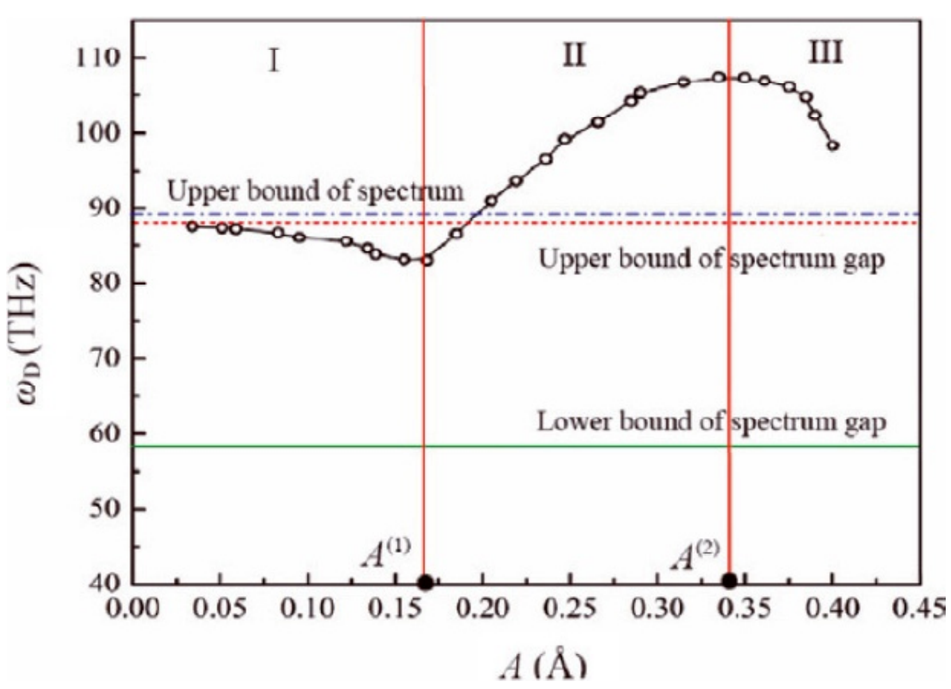

Fig. 16. Dependence of the frequency ω_D of the DB on the amplitude *A*. The curve is divided into three regions where the DB exhibits different types of anharmonicity. Reprinted with the permission from B. Liu, J.A. Baimova, K. Zhou, S.V. Dmitriev, X. Wang and H. Zhu // *J. Phys. D: Appl. Phys*. **46** (2013) 305302, © 2013 IOP Publishing.

type anharmonicity of the DBs in graphane in the entire range of DB amplitudes. From the comparison of MD [54] and *ab initio* [55] results it was concluded, that the MD simulation of DBs in graphane, performed using the AIREBO potential, gives an adequate estimation of DB frequency only for small

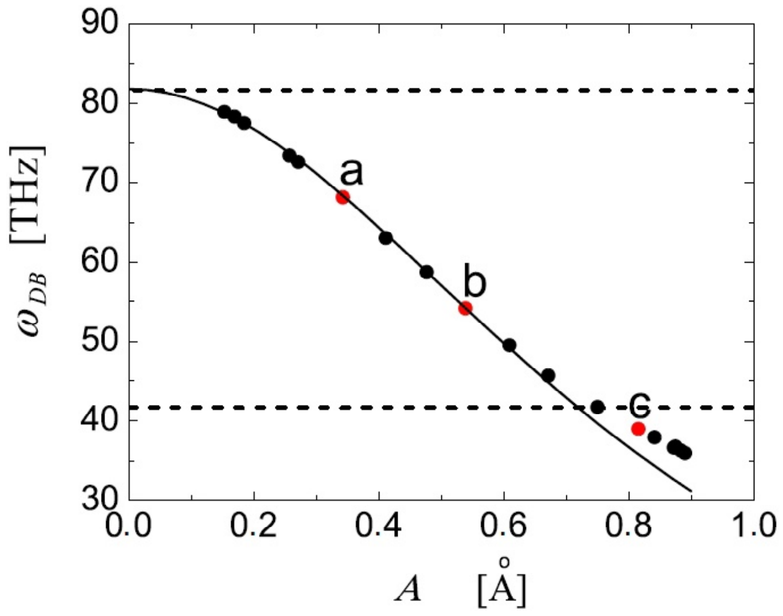

Fig. 17. DB frequency as the function of amplitude from *ab initio* simulation (scattered data). Horizontal dashed lines show the edges of gap in the DOS, ω_L and ω_H. Reprinted with the permission from G.M. Chechin, S.V. Dmitriev, I.P. Lobzenko and D.S. Ryabov // *Phys. Rev. B* **90** (2014) 045432, © 2014 American Physical Society.

amplitudes and shows a dramatic error for large amplitudes.

The understanding of the limitations for MD method also can be found in [30]. In Fig. 18 the kinetic energy of the hydrogen atoms as the function of time is shown for benzene. The corresponding excitation energy is ΔE=0.1391 eV and as can be seen from Fig. 18 it remains mostly localized at the site of the initial displacement from the equilibrium. A small part goes to the rest of the atoms but the DB which is now created remains stable and prevents energy propagation (at least for simulation times up to ns). The specific example of DB in benzene demonstrates classical DB in an “ideal” situation, but at the same time it forces one to confront with the limitations of classical vibrations. Quantum mechanically, it corresponds to an excitation lower in energy than the first excited vibrational state. The zero-point motion was not taken into account in this case. If one tries to relate to quantum mechanics, it should be viewed as a combination of the fundamental and excited states. The fact that DBs are observed in such small energies demonstrates that using the harmonic normal modes obtained from the second-order expansion of the energy around its classical equilibrium state is not correct. Using a semiclassical quantization of classical DBs would also be incorrect because the zero-point motion in the quantum ground-state energy of the molecule would involve displacements larger than the classical DBs amplitudes. A correct approach would be to use a Hartree type of method in this case, in order to find the proper fundamental state.

The experimental evidence of local modes (mini DBs) in isolated hydrocarbon molecules is abundant. The special conditions for its excitations are low densities and temperatures, which exist in the interstellar medium. Independent of the detailed structure of interstellar dust (molecular, amorphous or crystalline structures), the consensus is that it is mainly composed of C-H systems. The existence of DBs was also shown for polyethylene chain [57]. In the localization region periodic contraction-extension of valence C-C bonds occurs, which is accompanied by decrease-increase of valence angles. The concentration of thermally activated DBs in the chain has to increase when temperature grows.

5. CONCLUSIONS

Understanding DBs in realistic models of crystals is crucial for a variety of phenomena in condensed matter physics, chemistry, biological physics and other disciplines. The aim of this review was to give the reader an introduction into the fascinating field of localizing energy by nonlinearity and discreteness, while discussing details of recent achievements. The concept of localized excitations or DBs was presented and their basic properties including dynamical and structural stability were reviewed. Detailed discussion of recent numerical observations and studies of discrete breathers in carbon and hydrocarbon nanostructures was presented.

In particular, DBs in graphene, GNRs, CNTs and fullerenes were discussed together with the special conditions for their excitations. For example, results obtained for GNRs may be useful in the studies of its tensile strength at finite temperatures. It is well known that in the systems supporting DBs at zero temperature, spontaneous excitation of DBs at thermal equilibrium can take place [77]. Since DBs can localize sufficiently large energy, about 1 eV it is likely that they can initiate cracks in the GNR under tensile load at finite temperatures. Appearance of defects on the DB sites also can have great importance for investigation of structural stability and fracture of carbon nanostructures [52].

Another intriguing question is the energy redistribution and exchange between DBs in clusters in graphene and graphane. Despite moving DBs were found in many other realistic systems [9], still there is no studies on this subject for carbon and hydrocarbon nanostructures.

Recently, hydrogen storage technologies have attracted considerable attention due to increasing demands for cleaner and safer energy sources. However, several difficulties must be overcome before the practical implementation of such technologies becomes feasible. Portability and safeness are critical issues regarding the utilization of hydrogen

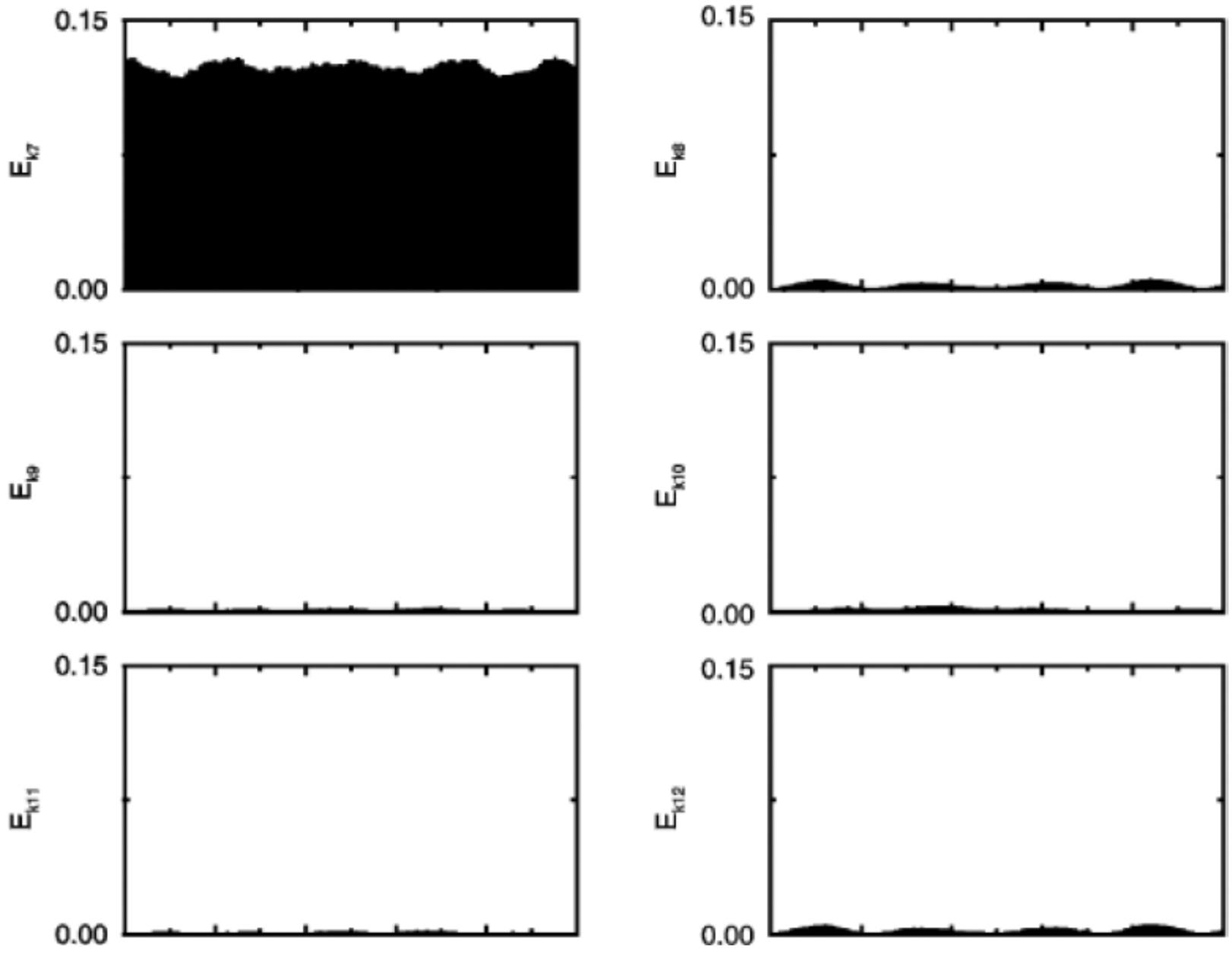

Fig. 18. The kinetic energy of H atoms, E_{ki} (eV) vs. time during the first 7 ps of the relaxation.

gas as a fuel. Particularly, carbon materials, for example graphene, provide a fertile playground for hydrogen storage due to their lightweight structure and high performance potential [80,83-87]. It was shown that graphene at low temperatures can easily absorb hydrogen and desorb it at high temperatures [80]. This suggests that the study of hydrogenation and dehydrogenation of graphene is very important for possible applications in electronics, spintronics and hydrogen storage. DBs in hydrocarbon structures definitely can be considered as one of the possible mechanisms for thermally activated dehydrogenation.

As an important open problem let us mention the study of DBs in carbon and hydrocarbon materials in the far-from-equilibrium states, e.g., under external high-frequency driving, in the presence of large temperature gradients, under irradiation etc.

AKNOWLEDGEMENT

JAB gratefully thanks Scholarship of the President of the Russian Federation for young scientists and PhD students SP-4037.2015.1. KEA is grateful for financial assistance from the President Grant of young scientists support (grant ¹ MK-5283.2015.2). IPL gratefully thanks financial support from the grant of Russian Science Foundation 14-13-00982. This work was partly supported (for SVD) by the Tomsk State University Academic D.I. Mendeleev Fund Program. The simulations were partly carried out on the supercomputer of RAS Supercomputer Center.

REFERENCES

[1] S.R. Bickham, S.A. Kiselev and A.J. Sievers // *Phys. Rev. B* **47** (1993) 14206.
[2] S.A. Kiselev, S.R. Bickham and A.J. Sievers // *Phys. Rev. B* **50** (1994) 9135.
[3] V.M. Burlakov, S.A. Kiselev and V.N. Pyrkov // *Phys. Rev. B* **42** (1990) 4921.
[4] M. Sato and A.J. Sievers // *Phys. Rev. B* **71** (2005) 214306.
[5] J.L. Marín, J.C. Eilbeck and F.M. Russell // *Phys. Lett. A* **248** (1998) 225.
[6] S. Flach, K. Kladko and C.R. Willis // *Phys. Rev. E* **50** (1994) 2293.
[7] I.A. Butt and J.A. Wattis // *J. Phys. A* **39** (2006) 4955.
[8] I.A. Butt and J.A. Wattis // *J. Phys. A* **40** (2007) 1239.
[9] A.A. Kistanov, S.V. Dmitriev, A.P. Chetverikov and M.G. Velarde // *Eur. Phys. J. B* **87** (2014) 211.
[10] S.V. Dmitriev, L.Z. Khadeeva, A.I. Pshenichnyuk and N.N. Medvedev // *Phys. Solid State.* **52** (7) (2010) 1499.

[11] S. A. Kiselev and A. J. Sievers // *Phys. Rev. B* **55**, 5755 (1997);
[12] N. K. Voulgarakis, G. Hadjisavvas, P. C. Kelires and G. P. Tsironis // *Phys. Rev. B* **69** (2004) 113201.
[13] L.Z. Khadeeva and S.V. Dmitriev // *Phys. Rev. B* **81** (2010) 214306.
[14] A. S. Dolgov // *Sov. Phys. Solid State* **28** (1986) 907.
[15] A. J. Sievers and S. Takeno // *Phys. Rev. Lett.* **61** (1988) 970.
[16] J. B. Page // *Phys. Rev. B* **41** (1990) 7835.
[17] R. S. MacKay and S. Aubry // *Nonlinearity* **7** (1994) 1623.
[18] S. Flach and C. R. Willis // *Phys. Rep*. **295** (1998) 181.
[19] S. Flach and A. V. Gorbach // *Phys. Rep*. **467** (2008) 1.
[20] E. Trias, J. J. Mazo and T. P. Orlando // *Phys. Rev. Lett.* **84** (2000) 741.
[21] J. W. Fleischer, M. Segev, N. K. Efremidis and D. N. Christodoulides // *Nature (London)* **422** (2003) 147.
[22] U. T. Schwarz, L. Q. English and A. J. Sievers // *Phys. Rev. Lett*. **83** (1999) 223.
[23] A. Trombettoni and A. Smerzi // *Phys. Rev. Lett*. **86** (2001) 2353.
[24] B. Eiermann, Th. Anker, M. Albiez, M. Taglieber, P. Treutlein, K.-P. Marzlin and M.K. Oberthaler // *Phys. Rev. Lett.* **92** (2004) 230401.
[25] M. Sato, S. Imai, N. Fujita, W. Shi, Y. Takao and Y. Sada // *Phys. Rev. E* **87** (2013) 012920.
[26] M. Spletzer, A. Raman, A. Q. Wu, X. Xu and R. Reifenberger // *Appl. Phys. Lett.* **88** (2006) 254102.
[27] J.Wiersig, S. Flach and K.H. Ahn // *Appl. Phys. Lett.* **93** (2008) 222110.
[28] L. Q. English, F. Palmero, P. Candiani, J. Cuevas, R. Carretero-Gonzalez, P. G. Kevrekidis and A. J. Sievers // *Phys. Rev. Lett.* **108** (2012) 084101.
[29] G. Kopidakis and S. Aubry // *Physica D* **130** (1999) 155.
[30] S. Aubry, G. Kopidakis, A.M. Morgante and G. Tsironis // *Physica B* **296** (2001) 222.
[31] H.-S. P. Wong and D. Akinwande, *Carbon Nanotube and Graphene Device Physics* (Cambridge University Press, Cambridge, 2011).
[32] M. I. Katsnelson, *Graphene: Carbon in Two Dimensions.* (Cambridge University Press, Cambridge, 2012).
[33] K. S. Novoselov, V. I. Fal'ko, L. Colombo, P. R. Gellert, M. G. Schwab and K. Kim // *Nature* **490** (2012) 192.
[34] M.F.L. De Volder, S.H. Tawfick, R.H. Baughman and A.J. Hart // *Science* **339** (2013) 535.
[35] Q. Zhang, J.-Q. Huang, W.-Z. Qian, Y.-Y. Zhang and F. Wei // *Small* **9** (2013) 1237.
[36] I.A. Ovid'ko // *Rev. Adv. Mater. Sci.* **32** (2012) 1.
[37] I.A. Ovid'ko // *Rev. Adv. Mater. Sci.* **34** (2013) 1.
[38] Y. Yamayose, Y. Kinoshita, Y. Doi, A. Nakatani and T. Kitamura // *Europhys. Lett.* **80** (2007) 40008.
[39] E.A. Korznikova, J.A. Baimova and S.V. Dmitriev // *Europhys. Lett.* **102** (2013) 60004.
[40] J.A. Baimova, S.V. Dmitriev and K. Zhou // *Europhys. Lett.* **100** (2012) 36005.
[41] E.A. Korznikova, Y.A. Baimova, S.V. Dmitriev, R.R. Mulyukov and A.V. Savin // *JETP Lett.* **96** (2012) 222.
[42] L.Z. Khadeeva, S.V. Dmitriev and Yu.S. Kivshar // *JETP Lett*. **94** (2011) 539.
[43] Y. Doi and A. Nakatani // *Procedia Engineering* **10** (2011) 3393.
[44] Y. Doi and A. Nakatani // *Journal of Solid Mechanics and Materials Engineering* **6**(1) (2012) 71.
[45] Y. Yamayose, Y. Kinoshita, Y. Doi, A. Nakatani and T. Kitamura // *Europhys. Lett.* **80** (2007) 40008.
[46] M. Vandescuren, P. Hermet, V. Meunier, L. Henrard and Ph. Lambin // *Phys. Rev. B* **78** (2008) 195401.
[47] W. Liang, G.M. Vanacore and A.H. Zewail // *PNAS* **111** (2014) 5491.
[48] Y. Kinoshita, Y. Yamayose, Y. Doi, A. Nakatani and T. Kitamura // *Phys. Rev. B* **77** (2008) 024307.
[49] A.V. Savin and Y.S. Kivshar // *Europhys. Lett*. **82** (2008) 66002.
[50] T. Shimada, D. Shirasaki, Y. Kinoshita, Y. Doi, A. Nakatani and T. Kitamura // *Physica D* **239** (2010) 407.
[51] I. Akimoto and K. Kanno // *J. Phys. Soc. Japan* **71** (2002) 630.
[52] T. Shimada, D. Shirasaki and T. Kitamura // *Phys. Rev. B* **81** (2010) 035401.
[53] A.V. Savin and Y.S. Kivshar // *Phys. Rev. B* **85** (2012) 125427.
[54] B. Liu, J.A. Baimova, K. Zhou, S.V. Dmitriev, X. Wang and H. Zhu // *J. Phys. D: Appl. Phys*. **46** (2013) 305302.

[55] G.M. Chechin, S.V. Dmitriev, I.P. Lobzenko and D.S. Ryabov // *Phys. Rev. B* **90** (2014) 045432.
[56] G. Kopidakis and S. Aubry // *Physica B* **296** (2001) 237.
[57] A.V. Savin and L.I. Manevitch // *Phys. Rev. B* **67** (2003) 144302.
[58] A. J. Stone and D. J. Wales // *Chem. Phys. Lett.* **128** (1986) 501.
[59] A.V. Savin and Yu. S. Kivshar // *Europhys. Lett.* **89** (2010) 46001.
[60] A.V. Savin and Yu. S. Kivshar // *Phys. Rev. B* **81** (2010) 165418.
[61] A.V. Savin and Yu. S. Kivshar // *Europhys. Lett.* **82** (2008) 66002.
[62] A.V. Savin, Yu. S. Kivshar and B. Hu // *Phys. Rev. B* **82** (2010) 195422.
[63] D.W. Brenner // *Phys. Rev. B* **42** (1990) 9458.
[64] S. Plimpton // *J. Comput. Phys*. **117** (1995) 1.
[65] S.J. Stuart, A.B. Tutein and J.A. Harrison // *J. Chem. Phys*. **112** (2000) 6472.
[66] J. Zhou and J. Dong // *Appl. Phys. Lett*. **91** (2007) 173108.
[67] J. Zhou and J. Dong // *Physics Letters A* **372** (2008) 7183.
[68] M. Xia, Z. Su, Y. Song, J. Han, S. Zhang and B. Li // *Eur. Phys. J. B* **86** (2013) 344.
[69] T. Zhu and J. Li // *Progr. Mater. Sci*. **55** (2010) 710.
[70] J. A. Baimova, S.V. Dmitriev and K. Zhou // *Superlattices and Microstructures* **54** (2013) 39.
[71] S.V. Dmitriev, J.A. Baimova, A.V. Savin and Yu.S. Kivshar // *Comp. Mater. Sci.* **53** (2012) 194.
[72] J.A. Baimova, S.V. Dmitriev, K. Zhou and A.V. Savin // *Phys. Rev. B* **86** (2012) 035427.
[73] Y.A. Baimova, S.V. Dmitriev, A.V. Savin and Y.S. Kivshar // *Phys. Solid State* **54** (2012) 866.
[74] S.V. Dmitriev, Y.A. Baimova, A.V. Savin and Y.S. Kivshar // *JETP Lett.* **93** (2011) 571.
[75] F. Liu, P. Ming and J. Li // *Phys. Rev. B* **76** (2007) 064120.
[76] M. Manley, A. Sievers, J. Lynn, S. Kiselev, N. Agladze, Y. Chen, A. Llobet and A. Alatas // *Phys. Rev. B* **79** (2009) 134304.
[77] L.Z. Khadeeva and S.V.Dmitriev // *Phys. Rev. B* **84** (2011) 144304.
[78] M.H.F. Sluiter and Y. Kawazoe // *Phys. Rev. B* **68** (2003) 085410.
[79] J.O. Sofo, A.S. Chaudhari and G.D. Barber // *Phys. Rev. B* **75** (2007) 153401.
[80] D.C. Elias, R.R. Nair, T.M. Mohiuddin, S.V. Morozov, P. Blake, M.P. Halsall, A.C. Ferrari, D.W. Boukhvalov, M.I. Katsnelson, A.K. Geim and K.S. Novoselov // Science **323** (2009) 610.
[81] G. M. Chechin and G. S. Bezuglova // *J. Sound Vib*. **322** (2009) 490.
[82] G. M. Chechin and I. P. Lobzenko // *Letters on materials* **4** (2014) 226.
[83] A.C. Dillon, K.M. Jones, T.A. Bekkedahl, C.H. Kiang, D.S. Bethune and M.J. Heben // *Nature* **386** (1997) 377.
[84] C. Liu, Y.Y. Fan, M. Liu, H.T. Cong, H.M. Cheng and M.S. Dresselhaus // *Science* **286** (1999) 1127.
[85] R. Strobel, L. Jorissen, T. Schliermann, V. Trapp, W. Schutz, K. Bohmhammel, G. Wolf and J. Garche // *J. Power Sources* **84** (1999) 221.
[86] R.T. Yang // *Carbon* **38** (2000) 623.
[87] W.C. Xu, K. Takahashi, Y. Matsuo, Y. Hattori, M. Kumagai, S. Ishiyama, K. Kaneko and S. Iijima // *Int. J. Hydrogen Energy* **32** (2007) 2504.